J Nanostruct 14(1): 38-47, Winter 2024

RESEARCH PAPER

Polyurethane/Silver Nanoparticle Composite Thermal Behavior and Electrical Conductivity Enhancement Based on Chalconic Moiety

Rand Sameer Hanoon, Ali Kareem A. Al-Lami, Ahmed M. Abbas *

Department of Chemistry, College of Science, University of Misan, Maysan, Iraq

ARTICLE INFO

Article History:
Received 14 September 2023
Accepted 21 December 2023
Published 01 January 2024

Keywords:
Electrical conductivities
Nanoparticle composite
Polyurethane

ABSTRACT

The study work includes the synthesis and characterization of three monomers based on a chalconic moiety containing hydroxyl groups in the para position. A condensation reaction was performed by combining MDI, TDI, and HDI with three monomers, which resulted in the effective synthesis of nine novel polyurethanes. Routine techniques such as Fourier-Transform Infrared (FTIR), Nuclear Magnetic Resonance (NMR) spectroscopy, X-ray diffraction (XRD), and Transmission Electron Microscopy (TEM) micrographs were used to determine the structures and properties of the prepared compounds. Additionally, the thermal behavior of the compounds was evaluated using thermogravimetric analysis (TG) analyses. The electrical conductivities of polyurethane were developed by incorporating conductive nanoparticles, such as silver nanoparticles, into the newly synthesized polyurethane nanocomposites. These nanocomposites exhibit good conducting performance when a mixture of silver nanoparticles and sodium chloride is incorporated into the polyurethanes. When nano silver and NaCl were used as dopants in PBT, the material exhibited 199.77 S/cm of the maximum electrical conductivity measured.

How to cite this article
Hanoon R S., A. Al-LamiA K., Abbas A M.. Polyurethane/Silver Nanoparticle Composite Thermal Behavior and Electrical Conductivity Enhancement Based on Chalconic Moiety. J Nanostruct, 2024; 14(1):38-47. DOI: 10.22052/JNS.2024.01.004

INTRODUCTION

The scientific and economic interest in polyurethane polymers is high, and their use in industry is on the rise [1, 2]. Polyurethane products and many nanomaterials, which have been widely used to produce composites or as reinforcers of thermoplastic and thermoset polymer matrices in textile, car, packaging, civil construction industry applications, and so on, are most widely used in the transportation sector[1–5]. Polyurethanes' low cost high resilience and lifetime make them a good choice for many medical applications [6]. This quality of polymeric materials has made them superior to their more conventional counterparts, such as ceramics and metals. Epoxies, unsaturated polyesters, and phenolics are all examples of thermoplastic and thermoset polymers; polyurethanes are in the same family. In a highly exothermic reaction, an isocyanate group (-N=C=O) is converted into a urethane linkage by reacting with an alcohol (-OH). The polyaddition reaction generates polyurethanes, and the core of an inflated foam can reach temperatures of 150–70 °C. In recent years, several organic successive

* *Corresponding Author Email: ahmedjmn@uomisan.edu.iq*

polymers have been discovered, that can become electrically conductive through doping with either acceptors or strong electron donors. Then the two scientists Heeger and MacDiarmid noticed for the first time that the conductivity of polyacetylene increases significantly when the polymer is treated with an oxidizing or reducing agent [7-10].

As a result of their antibacterial properties, optical qualities, electrical conductivities and potential antioxidant action, polymer-silver composites have seen extensive use [11, 12] Superior electrical properties, high stability, and antibacterial uses make many materials such as liquid crystals, silver, zinc oxide and iron oxide nanoparticles modified with diverse polymers of great interest [13- 19]. Conductive fibers with high electrical conductivity while also offering great flexibility and stretchability require the mixing of conductive fillers in a soft polymer. Additionally, there are typically trade-off features between conductivity and stretchability in conductive composite materials. Numerous articles have been published on the topic of synthesizing polyurethane and polyurethane-zinc composites. However, there is a lack of research into the production of polyurethane-silver composites.

As a chain extender in polyurethane synthesis, we have designed and synthesized chalconic units in the present study. The incorporation of chalconic units into the structure boosted the resulting PU's thermal stability. This led us to develop novel, previously unreported polyurethane and polyurethane-silver composites. Silver composites based on polyurethane were newly created by dispersing silver particles in dimethylformamide (DMF) in a simple technique. Silver nanoparticles stabilized by polyurethanes have been shown to significantly enhance conductivity measurements and are hence of considerable interest. Fourier-transform infrared spectroscopy (FTIR), nuclear magnetic resonance (NMR) spectroscopy (XRD), and thermogravimetric analysis (TGA) have all been used to analyze these produced substances. Composites' morphological characteristics were analyzed using scanning electron microscopy with energy dispersive spectroscopy. The Ossila four-point probe approach with the T2001A3 electrometer was used to determine the conductivity values of the composites. There is a wide variety of uses that could benefit from these materials' novel structures, characteristics, and morphological models.

MATERIALS AND METHODS

Aldrich-Sigma compounds Co. provided all compounds, which were used in their original form. Using a Shimadzu FT-IR 8400s spectrometer, we performed a Fourier transform infrared (FT-IR) spectrum study from 400 to 4000 cm^{-1}. Using deuterated DMSO as the solvent and TMS as an internal reference, 500 MHz ^1H NMR spectra were obtained on a Bruker DMX-300 spectrometer. The thermogravimetric analysis (TGA) was performed using an SDT-Q600 to determine the degradation properties of the produced polymers. Under a nitrogen environment, temperatures were measured from 25 to 800 °C at a rate of 20 °C/min. Using a Cu K radiation source at 30 kV and 20 mA at ambient temperature, powder X-ray diffraction (XRD) was carried out on a HAOYUAN Dx2700BH Dandong. The radiation source's wavelength was 1.5406. Conductivity measurements of composites were determined with Ossila four-point probe technique using a T2001A3 electrometer.

Synthesis of Monomer A

In a round-bottomed flask, 20 mL of methanol, 40 mmol of *p*-hydroxybenzaldehyde, and 45 mmol of anhydrous $CaCl_2$ were combined with 3.2 mmol (0.4 mL) of $BF_3 \bullet Et_2O$. A temperature of 50 degrees Celsius was reached in the mixing process. After waiting 12 hours, 20 mmol of acetone (about 1.5 mL) was added to 3.5 mL of methanol and added to the reaction mixture. 500 mL of water was added to the reaction mixture. The obtained precipitate was dried in a vacuum oven at 60 degrees Celsius for 12 hours (yield: 95%) [14]. ^1H NMR (500 MHz, DMSO-d6) δ 10.09 (s, 2H), 7.68−7.62 (m, 4H), 7.16−7.06 (m, 4H), 6.88−6.55 (m, 4H,). FTIR (KBr) ν_{max} = 3290,1630, 1593, 1512 cm^{-1}.

Synthesis of Monomer B

In a round-bottomed flask, we combined 20 mmol (2.44 g) of *p*-hydroxybenzaldehyde, 20 mmol (2.72 g) of *p*-hydroxy acetophenone, and 27 mmol (3.0 g) of anhydrous $CaCl_2$ with 0.4 mmol (0.05 mL) of $BF_3 \bullet Et_2O$ and 10 mL of methanol. After 10 hours of reaction at 50 degrees Celsius, the mixture was diluted by adding 500 millilitres of water. The precipitate was gathered and then dried under vacuum at 60 degrees Celsius for 12 hours (yield: 95 %) [20]. ^1H NMR (500 MHz, DMSO-d6) δ 10.35 (s, 1H), 10.03 (s, 1H), 8.05−8.03 (d, 2H), 7.72−7.59 (m, 4H), 6.89−6.82 (m, 4H,). FTIR (KBr) ν_{max} = 3344, 1647, 1604,1542 cm^{-1}.

Synthesis of Monomer V

To a round-bottomed flask containing 10 mmol of vanilla, 10 mmol of *p*-hydroxy acetophenone, and 27 mmol of anhydrous $CaCl_2$ were added 0.8 mmol of $BF_3 \bullet Et_2O$ (0.1 mL) and 15 mL of methanol. After 8 hours of reaction at 50 degrees Celsius, the mixture was diluted by adding 500 millilitres of water. For 12 hours at 80 degrees Celsius under vacuum, the precipitate was dried (yield 95%) [14]. ^{1}H NMR (500 MHz, DMSO-d6) δ 10.38 (s, 1H), 9.77 (s, 1H), 8.08−8.05 (d, 2H), 7.84−7.39 (m, 4H),7.26-7.25(d,1H), 6.97−6.81 (m, 2H,), 3.87 (s,3H). FTIR (KBr) ν_{max}= 3244, 1645, 1603,1591 cm^{-1}.

General synthesis of polyurethanes PAT, PBT, and PVT

6.3 mmol of suitable monomer and 10 mL of dimethylformamide (DMF) were added to a round-bottomed flask. While the solution was mixed with magnetic stirring, 6.3mmol of TDI was added and stirred well for 10 minutes at room temperature. The reaction temperature was increased to 60 ^{0}C for 4h. Gel formation was observed, and the precipitate was washed with methanol several times then collected and dried at 40 °C in vacuum for 4 h.

General synthesis of polyurethanes PAM, PBM, and PVM

6.3 mmol of suitable monomer and 10 mL of dimethylformamide (DMF) were added to a round-bottomed flask. While the solution was mixed with magnetic stirring, 6.3mmol of TDI was added and stirred well for 10 minutes at room temperature. The reaction temperature was increased to 60 ^{0}C for 4h. Gel formation was observed, and the precipitate was washed with methanol several times then collected and dried at 40 °C in vacuum for 4 h.

General synthesis of polyurethanes PAH, PBH, and PVH

6.3 mmol of suitable monomer and 10 mL of dimethylformamide (DMF) were added to a round-bottomed flask. While the solution was mixed with magnetic stirring, 6.3 mmol of HDI was added and stirred well for 10 minutes at room temperature. The reaction temperature was increased to 60 ^{0}C for 4h. Gel formation was observed, and the precipitate was washed with methanol several times then collected and dried at 40 °C in vacuum for 4 h.

Preparation of silver nanoparticles by sol-gel method

(0.001 M, 0.17 g) of silver nitrate $AgNO_3$ was added to a round-bottomed flask with 100 mL of deionized water, the mixture was heated with stirring at 90 °C, and then the flask was covered with aluminium foil to prevent oxidation of silver nitrate, (100 mL) of sodium citrate was added slowly, prepared by adding (0.01 g 0.26 M) sodium citrate to 100 ml of deionized water. The color solution changed from colorless to Pale yellow, the solution was put in a cold-water bath, and then drops of 10% NaOH were added with Continuous stirring until the pH reached (10-11). Then the precipitate was collected in a centrifuge machine at a speed of (5000 rpm). Then the deionized water was added, and the separation process was repeated twice to remove unreacted dissolved ions, the product was collected and dried at room temperature for two days away from light. The precipitate black powder is placed in plastic bottles with a capacity of (1.5 - 2.2 mL) [21].

Preparation of polyurethane-nano silver particle composite membranes

The polyurethane-nano silver particle composite was prepared by dissolving 0.05 g of polyurethane (PBT, PVT, and PVM) in 1 mL DMSO. To this solution, 0.1 g NaCl dissolved in deionized water was added. After that, 0.1g of silver nanoparticles were added. Then the mixture was sonicated in an ultrasonic bath (30 ^{0}C for 5 min). After the mixture becomes homogeneous, the mixture is placed on a glass slide and left until the solvent volatilizes, thus making it ready for electrical measurements.

RESULTS AND DISCUSSION

The synthetic route of polyurethane's series and the structures of monomers A, B and V are illustrated in Fig. 1. The solubility of the obtained polymers was tested in the commonly used organic solvents. The results show that polymers PAH, PBH and PVH are soluble poorly in polar solvents and PAT, PBT, and PVT are soluble well in some polar solvents like DMSO, and DMF. The solubility of polymer containing TDI moiety is higher than polymer containing HDI and MDI due to the presence of methoxy group in structure leading to the increase in the polarization of this polymer. Due to the poor solubility of polymers containing HDI and MDI in the solvent, its NMR

spectra could not be.

Spectral studies

^{1}H NMR spectra of PAT and PVT polyurethane prepared from Toluene Diisocyanate and dihydroxy chalcone in DMSO-d6 are demonstrated in Fig. 2. In general, the two signals observed at 1.98 and 2.199 ppm are assigned to Methyl groups on aromatic rings, two aromatic structures expected in absence of side reactions [22-25]. The two singlet signals observed at the most downfield region, δ=9.94 and 8.89 ppm, supported the presence of two N-H amide linking groups in the aromatic rings of TDI. Aromatic protons and Olefinic protons are observed within the chemical shift range of δ=8.43-6.32ppm. Singlet resonate at δ=4.74 ppm to the methoxy protons that are directly connected to an aromatic ring of vanillin in chalconic moiety. Proves that the polymerization reactions have occurred successfully and the amide groups NHCOO have formed in the structure of polymers.

FT-IR spectra of some polyurethane are shown in Fig. 3. The appearance of two new bands at 3200- 3300 and 1710-1720 cm^{-1} indicates the presence of NH and carbonyl groups, respectively in linking groups of polyurethane bands NHCOO. The analysis results of the resonance signals of the protons in the polymers and FT IR spectra are summarized:

P AT: Yellow solid; m.p 230-232 ^{0}C, yield 72 %, FT-IR (Nujol, ν_{max} in cm^{-1}): 3282 (N-H urethane **NH**COO), 3032 (C-H aromatic), 2920-2858 (C-H aliphatic), 1710 (C=O NH**CO**O), 1647 (C=O ketone), 1595 (C=C aromatic), 1600(C=C Olefine), 1543-1423(C=C aromatic), 1269(C-N). ^{1} H NMR (400 MHz, DMSO-d6, TMS, ppm) δ 9.02 (s, 1H, N-Ha), 8.89 (s, 1H, N-Hb), 8.43−6.32 (m, 16H, Ar-H and -HC=CH-), 2.14 (m, 3H, CH_3), 1.98(m, 3H, CH_3).

P BT. A yellow solid; m.p 200-212 ^{0}C, FT-IR

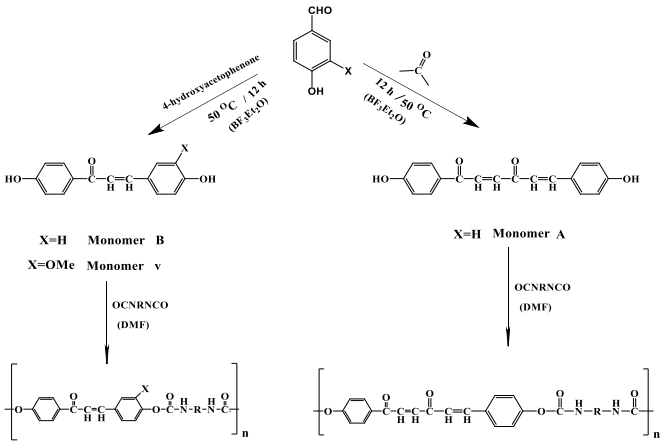

R	X=H	X=OMe
—$(CH_2)_6$—	PBH	PVH
	PBT	PVT
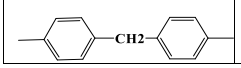	PBM	PVM

R	X=H
—$(CH_2)_6$—	PAH
	PAT
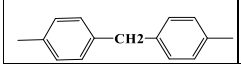	PAM

Fig. 1. Preparation of the polyurethane's series

(Nujol, ν_{max} in cm^{-1}): 3387 (N-H urethane **NH**COO), 3020 (C-H aromatic), 2920-2858 (C-H aliphatic), 1735 (C=O urethane NH**CO**O), 1654 (C=O ketone), 1597 (C=C Olefine), 1504-1423(C=C Ar), 1215(C-N). ^{1}H NMR (400 MHz, DMSO-d6, TMS, ppm) δ 9.41 (s, 1H, N-Ha), 9.12 (s, 1H, N-Hb), 8.61−6.82 (m, 16H, Ar-H and -HC=CH-), 2.61 (m, 3H, CH_3), 2.21(m, 3H, CH_3).

P VT. A yellow solid; m.p 230-232^{0}C, FT-IR (Nujol, ν_{max} in cm^{-1}): 3292 (N-H urethane **NH**COO), 3070 (C-H aromatic), 2920-2856 (C-H aliphatic), 1705 (C=O urethane NH**CO**O), 1649 (C=O ketone), 1597

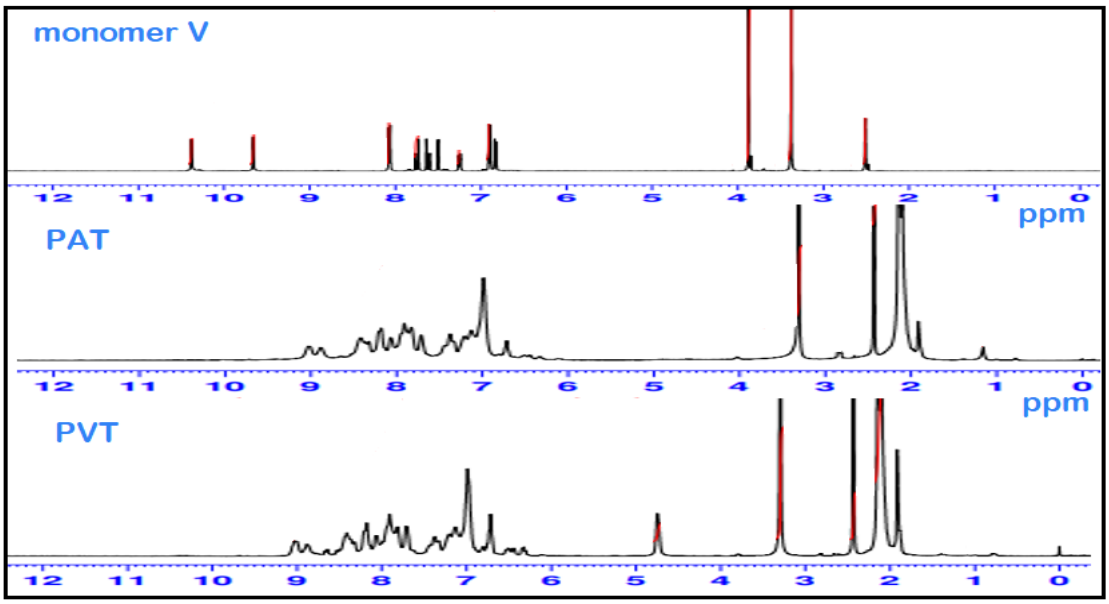

Fig. 2. ^{1}H NMR spectra of some of the compounds

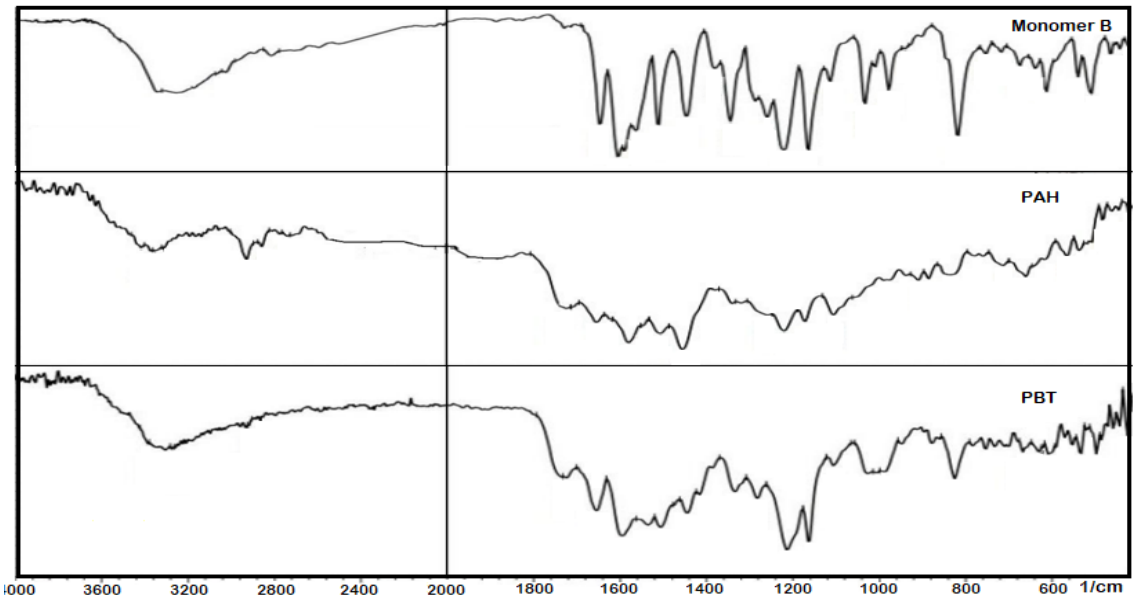

Fig. 3. FT-IR spectra of some of the compounds

(C=C Olefine), 1539-1413 (C=C aromatic), 1219 (C-N). ^{1}H NMR (400 MHz, DMSO-d6, TMS, ppm) δ 9.02 (s, 1H, N-Ha), 8.99 (s, 1H, N-Hb), 8.43−6.32 (m, 16H, Ar-H and -HC=CH-), 4.74 (s, 3H, OCH_3), 2.14 (m, 3H, CH_3), 1.88(m, 3H, CH_3).

PAM. A yellow solid; m.p, 240 ^{0}C decompose, FT-IR (Nujol, ν_{max} in cm^{-1}): 3367 (N-H urethane **NH**COO), 3028 (C-H aromatic), 2900-2839 (C-H aliphatic), 1720 (C=O NH**CO**O), 1674 (C=O ketone), 1597 (C=C Olefine), 1508-1423(C=C aromatic), 1230(C-N).

P BM. A yellow solid; m.p 223-225 ^{0}C, FT-IR (Nujol, ν_{max} in cm^{-1}): 3352 (N-H urethane **NH**COO), 3026 (C-H aromatic), 2900-2837 (C-H aliphatic), 1720 (C=O urethane NH**CO**O), 1671 (C=O ketone), 1508 (C-H aromatic), 1597 (C=C Olefine), 1431-149(C=C aromatic), 1230(C-N).

PVM. A yellow solid; m.p 210^{0}C, FT-IR (Nujol, ν_{max} in cm^{-1}): 3352 (N-H urethane **NH**COO), 3024 (C-H aromatic), 2900-2840 (C-H aliphatic), 1750 (C=O urethane NH**CO**O), 1670 (C=O ketone), 1597 (C=C Olefine), 1573-1408 (C=C aromatic), 1230(C-N).

P AH. A yellow solid; m.p 210-212 ^{0}C, FT-IR (Nujol, ν_{max} in cm^{-1}): 3414 (N-H urethane **NH**COO), 3070 (C-H aromatic), 2924-2854 (C-H aliphatic), 1720 (C=O urethane NH**CO**O), 1651 (C=O ketone), 1573 (C=C aromatic), 1615 (C=C Olefine), 1543-1423(C=C aromatic), 1215 (C-N).

PBH. A yellow solid; m.p 213-215^{0}C, FT-IR (Nujol, ν_{max} in cm^{-1}): 3317 (N-H urethane **NH**COO), 3026 (C-H aromatic), 2927-2854 (C-H aliphatic), 1705 (C=O urethane NH**CO**O), 1662 (C=O ketone), 1610 (C=C Olefine), 1573 (C=C aromatic), 1531-1423(C=C aromatic), 1215(C-N).

PVH. A yellow solid; m.p 240^{0}C decompose FT-IR (Nujol, ν_{max} in cm^{-1}): 3363 (N-H urethane **NH**COO), 3066 (C-H aromatic), 2931-2854 (C-H aliphatic), 1739 (C=O urethane NH**CO**O), 1662 (C=O ketone), 1604 (C=C Olefine), 1573-1408 (C=C aromatic), 1203(C-N).

Thermal Stability of polyurethane

TGA was used to evaluate the thermal characterization of prepared polyurethanes, Fig. 4 shows the TGA curves in a nitrogen atmosphere with a heating rate of 20 ^{0}C $min^{-1.}$ In general, it was observed that the sequence of degradation

Table 1. TG data and assignments of prepared polyurethane

polymers	stage	Temperature range °C	Weight loss %	Total weight loss %
PAM	1st	40 - 90	2.722	57.85
	2nd	240 - 360	34.46	
	3rd	380 - 800	20.67	
PAT	1st	40 - 90	2.592	93.13
	2nd	220 - 340	77.99	
	3rd	380 - 800	12.55	
PAH	1st	40 - 85	1.820	37.06
	2nd	160 - 230	4.699	
	3rd	260 - 445	23.604	
	4th	490 -800	6.934	
PBM	1st	40 - 90	1.815	54.12
	2nd	230 - 340	31.95	
	3th	400 - 800	20.35	
PBT	1st	40 - 90	5.388	94.36
	2nd	190 - 310	66.45	
	3rd	330 - 800	22.43	
PBH	1st	90 - 140	0.780	74.42
	2nd	200 - 290	23.34	
	3rd	310 - 490	40.64	
	4th	500 -800	9.668	
PVM	1st	40 - 90	3.293	55.87
	2nd	240 - 310	27.86	
	3rd	350 - 800	24.12	
PVT	1st	55 - 100	3.356	90.15
	2nd	220 - 360	82.31	
	3rd	375 - 800	4.485	
PVH	1st	45 - 100	5.819	84.21
	2nd	180 - 320	39.22	
	3rd	350 - 800	39.19	

takes place in three stages depending on the mass loss in different temperature ranges. In the first stage, these polymers start with slight mass loss owing to the water molecule below T=100 °C and then fragments of the backbone and low molecular weight oligomers [26,27]. TGA curves show that the polyurethane PAH has the highest stability among prepared polymers, the initial step of degradation at 260 – 445 ^{0}C a corresponding mass loss of 23%, leaving a total residual mass of about 73%. While TGA curves of PBT, PAT and PVT polymers have the lowest stability and show three stages of decomposition, we see an initial step of degradation at 190 ^{0}C, 220 ^{0}C, and 220 ^{0}C corresponding with an abrupt total mass loss (94.36%, 93.13%, and 90.15%) respectively. The TGA data obtained from the TGA curves about the initial decomposition temperature and the mass

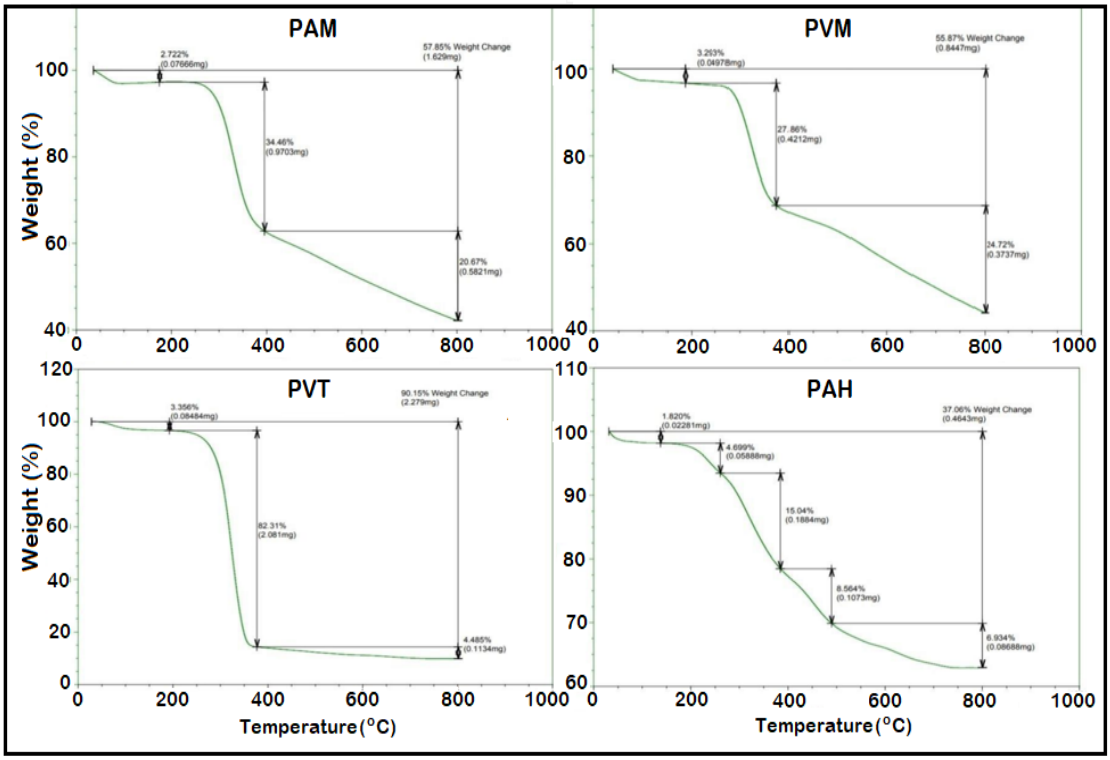

Fig. 4. TG curves of PAM, PVM, PVT and PAH polyurethane

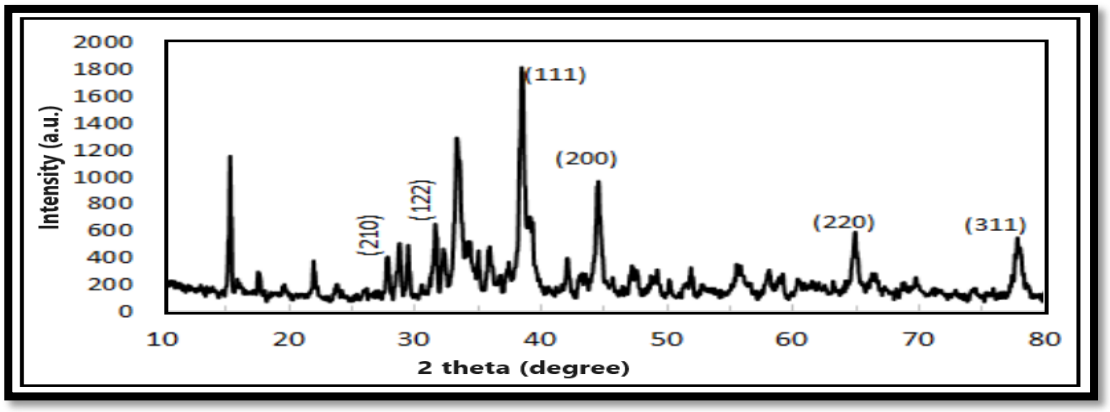

Fig. 5. XRD spectrum of AgNPs

loss at different temperatures are listed in Table 1.

The morphology and structure of polyurethane/ silver Nanocomposite

XRD patterns were considered one of the most important techniques in determining the phase formation and crystal structure of prepared silver nanoparticles. Fig. 5 shows the X-ray diffraction pattern of prepared Ag nanoparticles given six peaks. As shown, (210), (122), (111), (200), (220), and (311), planes are agreed with JCPDS No. 04-0783. On the other side, the crystal structure of the model is Cubic. The mean crystal size (L) for Ag nanoparticles was calculated by utilizing Scherrer's equations [28, 29].

$$L = k\lambda / \beta \cos\theta \quad (1)$$

Where k = 0.9 is the constant crystal lattice, λ, β and θ are indicated to shape constant, the wavelength of the radiation, Bragg diffraction angle, and full width at half maximum intensity (FWHM). The result indicates that it has a nano-size equal to 22.006 nm.

TEM images showed the formation of Ag nanosilver with prolate spheroidal phase structure Fig. 6. confirmed that the particles became irregular in shape and highly agglomerated upon silver. TEM images for Ag nano silver particles showed the presence of Ag+ on the surface of the samples

TEM micrographs of of B-M-Ag nanosilver are shown in Fig. 7. TEM study showed that the B-M-Ag nanosilver particles with 79 nm were formed with spherical geometry. Furthermore, a small

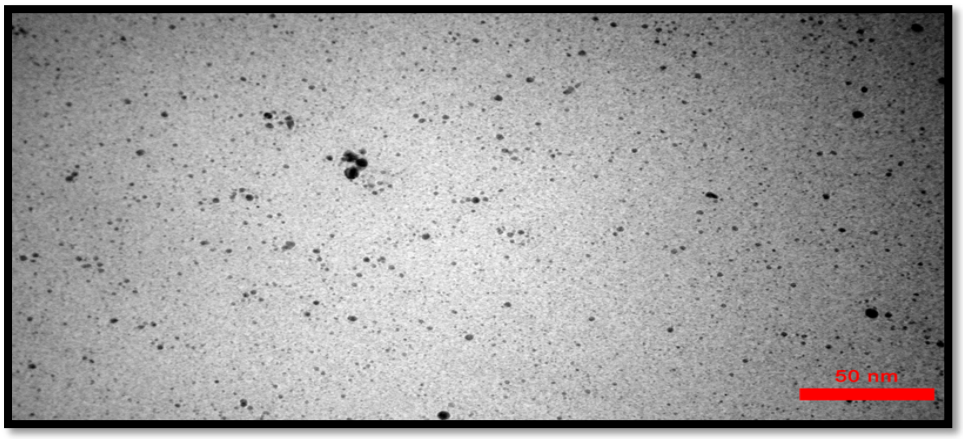

Fig. 6. TEM image of AgNPs

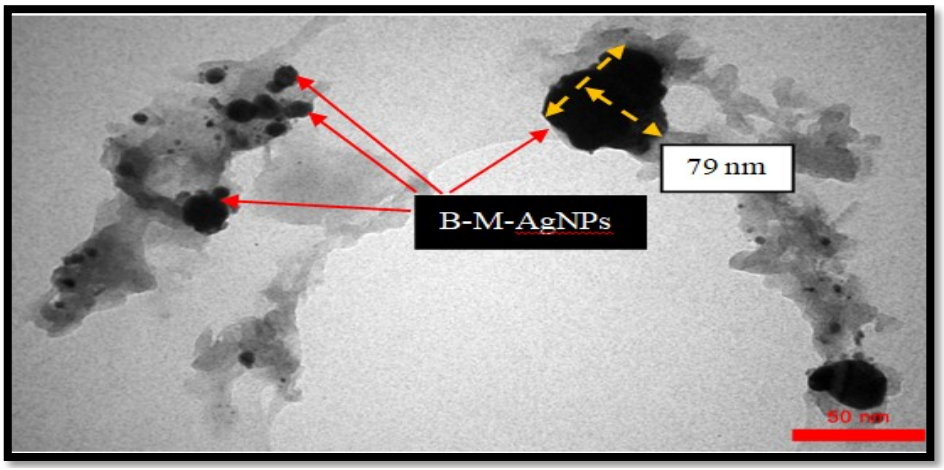

Fig. 7. TEM image of B-M-AgNPs

Table 2. electrical conductivity values(S/cm) of polyurethane and polyurethane /nano silver / NaCl composite

Polymers	electrical conductivity(S/cm)
PBM	0.00
PVM	0.00
PBT	0.00
PBT/ Ag NPs	188.64
PBT/ Ag NPs / NaCl	199.77
PBM/ Ag NPs / NaCl	198.16
PVM/ Ag NPs / NaCl	180.02

number of black spots were observed on the surface of the B-M-Ag nanosilver.

Electrical conductivity study

The electrical conductivities studies of polyurethane and polyurethane/Ag NPs/NaCl composite were carried out in membrane form. The four-probe method was used to carry out the study using an electrometer. The electrical conductivities of PBM, PVM, and PBT were found to be at 0 S/cm. Herein, it was seen that the electrical conductivities increased when the polymer was doped with silver. Table 2 shows the data for electrical conductivities of some prepared polyurethane and polyurethane/ Ag NPs /NaCl composite and it was found that the conductivity increases steadily with doping silver, conductivities of PBT/Nano silver were measured as 188.64 S/cm, the increase in electrical conductivity of polymers imply that the charge-transfer between polymers and dopant silver is formed without interrupting, the highest conductivity was observed in of PBT when use dopants nano silver and NaCl at 199.77 S/cm. The maximum conductivity values for PBM/Ag NPs/NaCl, and PVM/Ag NPs/NaCl, were found to be 198.16 and 180.02 S/cm respectively. According to these values, only small, noteworthy differences were found in electrical conductivity values of polyurethane /nano silver / NaCl composite [30,31].

CONCLUSION

This work presents a successful polyurethanes design for the generation of polyurethanes /AgNPs composite. Three monomers based on a chalconic units, and nine new polyurethanes have been successfully synthesized by condensation reaction with different types of isocyanates MDI, TDI and HDI. To develop the electrical conductivities of polyurethane, conductive nanoparticles, such as silver nanoparticles were added to the synthesized polyurethane nanocomposites exhibiting excellent conducting performance when a combination of silver nanoparticles, NaCl and prepared polyurethanes. The results of the TGA curves show that the obtained copolymers showed high thermal stability. The silver nanoparticle was investigated by XRD diffraction and TEM micrographs study showed the formation of Ag nano silver with prolate spheroidal phase structure and the B-M-Ag nano silver particles were formed with spherical geometry.

CONFLICT OF INTEREST

The authors declare that there is no conflict of interests regarding the publication of this manuscript.

REFERENCES

1. Das A, Mahanwar P. A brief discussion on advances in polyurethane applications. Advanced Industrial and Engineering Polymer Research. 2020;3(3):93-101.
2. Cao H, Liu R, Li B, Wu Y, Wang K, Yang Y, et al. Biobased rigid polyurethane foam using gradient acid precipitated lignin from the black liquor: Revealing the relationship between lignin structural features and polyurethane performances. Industrial Crops and Products. 2022;177:114480.
3. Yang J, Chen H, Yuan Y, Sarkar D, Zheng J. Synthesis and characterization of biocompatible polyurethanes for controlled release of hydrophobic and hydrophilic drugs. Frontiers of Chemical Science and Engineering. 2014;8(4):498-510.
4. Ali ZH, Al-Saady MA, Aldujaili NH, Rabeea Banoon S, Abboodi A. Evaluation of the Antibacterial Inhibitory Activity of Chitosan Nanoparticles Biosynthesized by Streptococcus thermophilus. Journal of Nanostructures. 2022;12(3):675-85.
5. Duarte LT, Habert AC, Borges CP. Preparation and morphological characterization of polyurethane/ polyethersulfone composite membranes. Desalination. 2002;145(1-3):53-59.
6. Carreño F, Gude MR, Calvo S, Rodriguez de la Fuente O, Carmona N. Design and development of icephobic coatings based on sol-gel/modified polyurethane paints. Materials Today Communications. 2020;25:101616.
7. Salazar-Bravo P, Del Angel-López D, Torres-Huerta AM, Domínguez-Crespo MA, Palma-Ramírez D, Brachetti-Sibaja

SB, Ferrel-Álvarez AC. Investigation of ZnO/Waterborne Polyurethane Hybrid Coatings for Corrosion Protection of AISI 1018 Carbon Steel Substrates. Metallurgical and Materials Transactions A. 2019;50(10):4798-4813.
8. Rahman MM. Polyurethane/Zinc Oxide (PU/ZnO) Composite—Synthesis, Protective Property and Application. Polymers. 2020;12(7):1535.
9. Hassan BA, Lawi ZKK, Banoon SR. Detecting the activity of silver nanoparticles, pseudomonas fluorescens and bacillus circulans on inhibition of aspergillus niger growth isolated from moldy orange fruits. Periódico Tchê Química. 2020;17(35):678-690.
10. Yağmur HK, Kaya İ. Synthesis and characterization of poly(urethane)/silver composites via in situ polymerization. Polym Compos. 2021;42(6):2704-2716.
11. Lawi ZK, Merza FA, Banoon SR, Jabber Al-Saady MA, Al-Abboodi A. Mechanisms of Antioxidant Actions and their Role in many Human Diseases: A Review. Journal of Chemical Health Risks. 2021;11.
12. Biao L, Tan S, Wang Y, Guo X, Fu Y, Xu F, et al. Synthesis, characterization and antibacterial study on the chitosan-functionalized Ag nanoparticles. Materials Science and Engineering: C. 2017;76:73-80.
13. Rabeea Banoon Z, Kareem A. Al-Lami A, Abbas AM, Al-Shakban M, A. A. Balboul B, Gad M, et al. Asymmetrical liquid crystals synthesis for effective sensing: Fluorescence investigations. Results in Chemistry. 2023;6:101166.
14. Al-Abboodi A, Albukhaty S, Sulaiman GM, Al-Saady MAAJ, Jabir MS, Abomughaid MM. Protein Conjugated Superparamagnetic Iron Oxide Nanoparticles for Efficient Vaccine Delivery Systems. Plasmonics. 2023;19(1):379-388.
15. Hassan SA, Almaliki MN, Hussein ZA, Albehadili HM, Banoon SR, Al-Abboodi A, Al-Saady M. Development of Nanotechnology by Artificial Intelligence: A Comprehensive Review. Journal of Nanostructures. 2023, 13(4): 915-932.
16. Banoon SR, Ghasemian A. The Characters of Graphene Oxide Nanoparticles and Doxorubicin Against HCT-116 Colorectal Cancer Cells In Vitro. J Gastrointest Cancer. 2021;53(2):410-414.
17. Lam WT, Babra TS, Smith JHD, Bagley MC, Spencer J, Wright E, Greenland BW. Synthesis and Evaluation of a Silver Nanoparticle/Polyurethane Composite That Exhibits Antiviral Activity against SARS-CoV-2. Polymers. 2022;14(19):4172.
18. Al-Saady AJ, Aldujaili NH, Banoon SR, Al-Abboodi A. Antimicrobial properties of nanoparticles in biofilms. Revis Bionatura 2022; 7 (4): 71.
19. Al-Abboodi A, Mhouse Alsaady HA, Banoon SR, Al-Saady M. Conjugation strategies on functionalized iron oxide nanoparticles as a malaria vaccine delivery system. Bionatura. 2021;3(3):2009-2016.
20. Zong R, Wang T. Significant Efficacy of Desiccants in the Synthesis of Distyryl Ketones/Chalcones Bearing Phenolic Hydroxyl Groups. Industrial & Engineering Chemistry Research. 2022;61(3):1294-1300.
21. Rabeea Banoon Z., A. Al-Lami A K., and Abbas A M. Synthesis and Studying the Optical Properties of Novel Zinc Oxide/a symmetric dimer Liquid Crystal Nanohybrid. Journal of Nanostructures. 2023;13(1): 159-172.
22. Sivakumar PM, Cometa S, Alderighi M, Prabhawathi V, Doble M, Chiellini F. Chalcone embedded polyurethanes as a biomaterial: Synthesis, characterization and antibacterial adhesion. Carbohydr Polym. 2012;87(1):353-360.
23. Pegoraro M, Galbiati A, Ricca G. 1H nuclear magnetic resonance study of polyurethane prepolymers from toluene diisocyanate and polypropylene glycol. J Appl Polym Sci. 2002;87(3):347-357.
24. Polo ML, Spontón ME, Jaramillo F, Estenoz DA, Meira GR. Linear segmented polyurethanes: I. A kinetics study. J Appl Polym Sci. 2017;135(4).
25. Mtimet I, Lecamp L, Kebir N, Burel F, Jouenne T. Green synthesis process of a polyurethane-silver nanocomposite having biocide surfaces. Polym J. 2012;44(12):1230-1237.
26. Čubrić G, Salopek Čubrić I, Rogale D, Firšt Rogale S. Mechanical and Thermal Properties of Polyurethane Materials and Inflated Insulation Chambers. Materials. 2021;14(6):1541.
27. Al-Lami AKA. Synthesis and characterization of hydrogen bonded liquid crystalline block copolymers based on a Schiff base moiety. Journal of Polymer Research. 2014;22(1).
28. Fakhri FH, Ahmed LM. Incorporation CdS with ZnS as Composite and Using in Photo-Decolorization of Congo Red Dye. Indonesian Journal of Chemistry. 2019;19(4):936.
29. Ruan K, Guo Y, Gu J. Interfacial thermal resistance of thermally conductive polymer composites. Thermally Conductive Polymer Composites: Elsevier; 2023. p. 197-232.
30. Velayutham TS, Abd Majid WH, Ng BK, Gan SN. Effect of oleic acid content and chemical crosslinking on the properties of palm oil-based polyurethane coatings. J Appl Polym Sci. 2012;129(1):415-421.
31. Yang X, Zhang J, Xia L, Xu J, Sun X, Zhang C, Liu X. Boron Nitride/Polyurethane Composites with Good Thermal Conductivity and Flexibility. Int J Mol Sci. 2023;24(9):8221.